https://doi.org/10.1007/s41230-018-8009-2

Nano-SiC_p particles distribution and mechanical properties of Al-matrix composites prepared by stir casting and ultrasonic treatment

***Shu-sen Wu, Du Yuan, Shu-lin Lü, Kun Hu, and Ping An**

State Key Lab of Materials Processing and Die & Mould Technology, Huazhong University of Science and Technology, Wuhan 430074, China

Abstract: Nano-ceramic particles are generally difficult to add into molten metal because of poor wettability. Nano-SiC particles reinforced A356 aluminum alloy composites were prepared by a new complex process, i.e., a molten-metal process combined with high energy ball milling and ultrasonic vibration methods. The nano particles were β-SiC_p with an average diameter of 40 nm, and pre-oxidized at about 850 °C to form an oxide layer with a thickness of approximately 3 nm. The mm-sized composite granules containing nano-SiC_p were firstly produced by milling the mixture of oxidized nano-SiC_p and pure Al powders, and then were remelted in the matrix-metal melt with mechanical stirring and treated by ultrasonic vibration to prepare the composite. SEM analysis results show that the nano-SiC particles are distributed uniformly in the matrix and no serious agglomeration is observed. The tensile strength and elongation of the composite with 2wt.% nano-SiC_p in as-cast state are 226 MPa and 5.5%, improved by 20% and 44%, respectively, compared with the A356 alloy.

Key words: metal matrix composites; SiC nanopaticles; A356 aluminum alloy; solid-liquid mixed casting; ultrasonic vibration

CLC numbers: TG146.21 **Document code:** A **Article ID:** 1672-6421(2018)03-203-07

Metal matrix composites (MMCs) with ceramic particles as reinforcement have higher specific strength, superior wear resistance and better dimensional stability than their matrix alloys [1]. It is believed that MMCs with micron-scale particles would have low ductility, but the nano-scale particles reinforced MMCs, termed as MMNCs, have enhanced ductility even with a very low volume fraction of nano particles [2-3]. Hence, MMNCs have gained great attention in scientific research and commercial application because of the demands for lightweight, high-modulus, and high-strength materials [4-5].

MMNCs are generally produced by two major methods, the solid state method and the liquid casting method. Usually, the fabrication process of the solid state method has a high cost [2, 6, 7]. The liquid method is economical, in which reinforcement particles are added directly to molten alloy by stirring and casting [8]. But the key problems during the addition of nano-sized ceramic particles into molten metal are wettability and dispersion. The wettability between nano-SiC particles and molten Al alloys is very poor due to the very high specific surface area of nano-particles. Therefore it is difficult to add nano-SiC particles into molten Al alloy with the common stirring method. Solid-liquid mixed casting is a casting method in which alloy powders with good wettability are added to the melt with mechanical stirring to fabricate high alloy material ingots. This method is proved to be feasible to fabricate MMCs by preparing composite granules which are made of ceramic particles and alloy powders with good wettability through mechanical alloying[9]. Ceramic particles are considered as alloying element when the casting method is applied to the fabrication of MMCs [9] and the weight fraction of reinforcement could rearch 5% [11] with μm-sized reinforcement. Su et al. [11] used aluminum powders as the carrier agent to fabricate 0.6%Al_2O_3/Al2024 composites. Mechanical alloying was achieved by ball-milling in which stearic acid was used as the process control agent (PCA) and resulted in composite granules with a diameter smaller than 100

***Shu-sen Wu**

Male, Ph. D, professor. His research interests focus mainly on Al alloys, Mg alloys and their composites.

E-mail: ssw636@hust.edu.cn

Corresponding author: Du Yuan, e-mail: dyuan879@hust.edu.cn

Received: 2018-02-01; Accepted: 2018-03-20

μm. Then mechanical stirring, which is similar to the fabrication process of the composites reinforced by μm-sized particles, is used to add the composite granules to the melt and fine dispersion of Al_2O_3 particles was achieved. There is a problem when solid-liquid mixed casting is applied to make MMNCs, that the size of composite granules would decrease rapidly during the melting process of pure Al, and traditional mechanical stirring is useless in uniformly dispersing particles in the melt on the macro level when the size of composite granules becomes too small. As a result, there exists agglomerations of nano-particles and the content of reinforcement in MMNCs is limited. Therefore, a new process for better dispersion is required.

In this work, Al MMNCs reinforced by dispersed SiC nanoparticles were fabricated by combining the processes of solid-liquid mixed casting and high-intensity ultrasonic vibration (UV). The mechanical alloying between nano-SiC_p and pure Al powders was achieved by high energy ball-milling (HBM) without PCA. The mm-sized composite granules, rather than μm-sized granules, were fabricated, and UV treatment was introduced to disperse the small agglomerations formed due to the near-complete melting of composite granules. The microstructure and mechanical properties of the nano-SiC_p/A356 were also studied to understand the effect of nanoparticles in as-cast composites.

1 Experimental procedure

The matrix material was A356 aloy, with compositions of 7% Si, 0.3% Mg, 0.19% Fe, and balanced Al. The reinforcements were β-SiC particles with an average diameter of 40 nm. Pure aluminum powders for preparing composite granules had an average diameter of 30 μm. There were two main procedures of the experiment, high energy ball-milling (HBM) for fabrication of nano-SiC_p/Al composite granules and solid-liquid mixed casting to fabricate MMNCs.

In order to prevent a reaction of SiC with Al melt, the pretreatment of nano-SiC_p was calcination at 850 ºC for 2 h, removing the imputies and gases on the surface of nano-SiC_p and forming a compact oxidation film. Then, the nano-particles were mixed with pure Al powders with a weight fraction of 6% of nano-SiC_p to fabricate nano-SiC_p/Al composite granules by dry HBM without PCA. The mixture of nano-SiC_p and pure Al powders was milled in a planetary mill at room temperature after the milling vessels was vacuumized and filled with stainless steel balls with diameter of 10 mm. Rotation speeds of the mill were sequential in a set of speeds kept about 150 rpm for 5 h, 200 rpm for 15 h and 300 rpm for 5 h.

A balanced amount of Al-24.5% Si master alloy ingot, pure Al and pure Mg blocks were melted in a graphite crucible to make about 2 kg composite at the end, according to the compositions of A356 alloy. The nano-SiC_p/Al composite granules were preheated at 250 ºC before adding into the melt. After the alloy was completely melted, mechanical stirring was applied as the melt was cooled down to 680 ºC, and the preheated nano-SiC_p/Al composite granules were added into the stirring vortex. The stirring speed was 250 rpm, stirring for 10 min after nano-SiC_p/Al composite granules were completely added to the melt. When the stirring process was over, the melt was heated up to 720 ºC and held for 30 min. In order to disperse SiC nano-particles in the melt, ultrasonic vibration (UV) with a 20 kHz, maximum 2.8 kW power output and a titanium alloy horn with 20 mm in diameter was introduced into the melt and kept for 3 min. After ultrasonic vibration processing, the composite melt was poured into a permanent steel mould and squeeze cast under a presure of 60 MPa. The mould was preheated to 250 ºC before pouring. Ingot-shape castings of MMNCs were obtained with a diameter of 30 mm and height of 100 mm. The tensile test samples and other samples were cut out from the ingot castings.

The tensile tests for unreinforced A356 and nanocomposite specimens were carried out with a Shimatsu AG-IC100KN tester at a strain rate of 1 $mm \cdot min^{-1}$ at room temperature. The diameter and gauge length of samples were 6 mm and 30 mm, respectively. Three specimens were tested at every data point and the average values were obtained. The distribution of the SiC nanoparticles were investigated with a DMM-480C optical microscope (OM), and a JEOL JSM-7600F scanning electron microscope (SEM) with JEM2100 (TEM). The samples were mechanically polished and etched using a solution with 0.5vol.% HF for 10 s.

2 Results and discussion

2.1 Morphology of pre-oxidized nano-SiC_p

High temperature is required during the stir-casting process of composite slurry, but it would increase the possibility of the reaction between SiC_p and the matrix aluminum to form Al_4C_3, as shown in Fig. 1. It is known that mechanical properties of SiC/Al composites will be degraded due to the formation of Al_4C_3, which is unstable in some environments such as water, methanol, HCl, etc [12].

Artificial oxidation of SiC to produce a SiO_2 layer on the

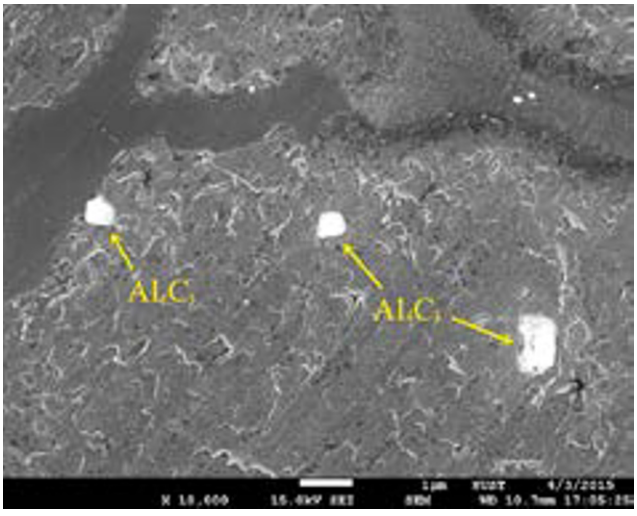

Fig. 1: SEM microstructures of nano-SiC_p/A356 composites with Al_4C_3 resulted from reaction of un-pretreated SiC_p with Al melt

surface of SiC has been proven to be effective in preventing the reaction[12]. Investigation on SiC_p oxidation at elevated temperatures shows that the oxidation increment of SiC_p, the dependence of the volume fraction and that of the thickness of SiO_2 layer on temperature are both parabolic [13]. Considering the SiC_p as regular spheres, the thickness of the SiO_2 layer defined as d could be estimated by Eqs. (1) and (2):

$$\frac{V_{SiO_2}}{V_{\Delta SiC}} = \frac{\frac{4}{3}\pi(R_3^3 - R_2^3)}{\frac{4}{3}\pi(R_1^3 - R_2^3)} = \frac{\frac{3\Delta w}{\rho_{SiO_2}}}{\frac{2\Delta w}{\rho_{SiC}}} \quad (1)$$

$$\frac{4}{3}\pi R_2^3\rho_{SiC} + \frac{4}{3}\pi(R_3^3 - R_2^3)\rho_{SiO_2} = \frac{m'}{m}\frac{4}{3}\pi R_1^3\rho_{SiC} \quad (2)$$

where R_1 is the average radius of SiC_p before pretreatment, R_3 is the average radius of SiC_p after pretreatment, R_2 is the average radius of a hypothetic sphere formed by the remaining part of pre-treated spheres with the exception of the SiO_2 layer, m and m' are the weight of SiC_p before and after pretreatment, respectively, and $\Delta w = m' - m$. Therefore, $d = R_3 - R_2$.

The density of β-SiC and amorphous state SiO_2 are 3.16 $g \cdot cm^{-3}$ and 2.196$g \cdot cm^{-3}$, respectively. R_1, the average radius of nano-SiC_p, is 20 nm. By weighing the SiC_p powders before and after oxidation, the value of the thickness of the SiO_2 layer can be estimated with Eqs. (1) and (2). The estimated thickness of oxidized SiC_p under different times are shown in the curve of Fig. 2. When the holding time is 2 h at 850 ºC, the thickness of SiO_2 layer is about 3 nm, which agrees well with the TEM measurement results, as shown in Fig. 3.

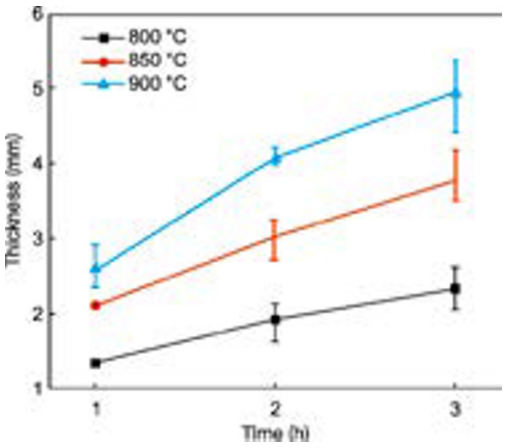

Fig. 2: Correlation of oxidation thickness and oxidation time of nano-SiC_p estimated by Eqs. (1) and (2)

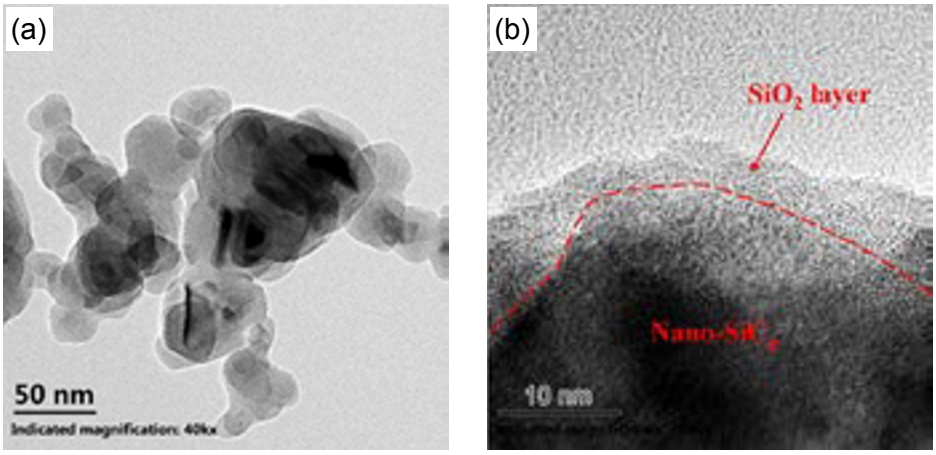

Fig. 3: TEM images of SiC_p after pre-oxidized at 850 °C for 2 h at low (a) and high (b) magnification

2.2 Morphologies and microstructures of nano-SiC_p/Al composite granules

Figure 4 shows the appearance of the composite granules which have an average diameter of 2 mm. The ball milling was taken between ductile (pure Al powder) material and brittle material (nano-SiC particles), and consisted 3 stages[14], as shown in Fig. 5. In the first stage (Fig. 5c), micro-forging existed between the Al powders and grinding balls. The Al powders were broken into cakes and slices, and the nano-SiC_p was stable in this stage. Then the lamellar structure would be formed by the slice-shaped Al and nano-SiC_p, while the caky Al would be transformed and broken further (Fig. 5d). The SiC_p was concentrated on the junctions between the two lamellar structures, and would adhere to the surfaces of the Al powders during the ball milling gradually in this stage. In the final stage, microcosmic routes for diffusion would exist due to the crystal defects produced by

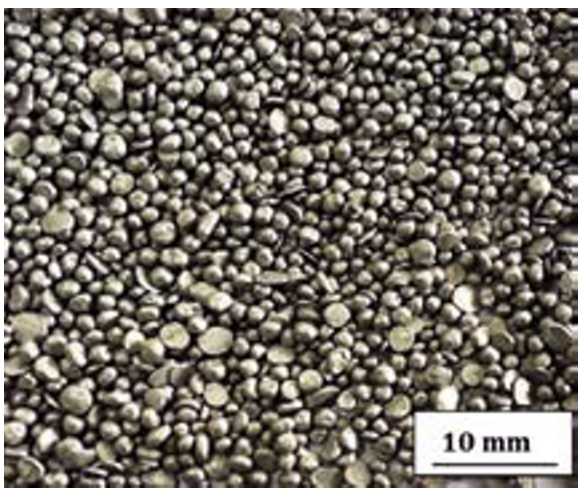

Fig. 4: Morphologies of composites granules with 6wt.% nano-SiC_p

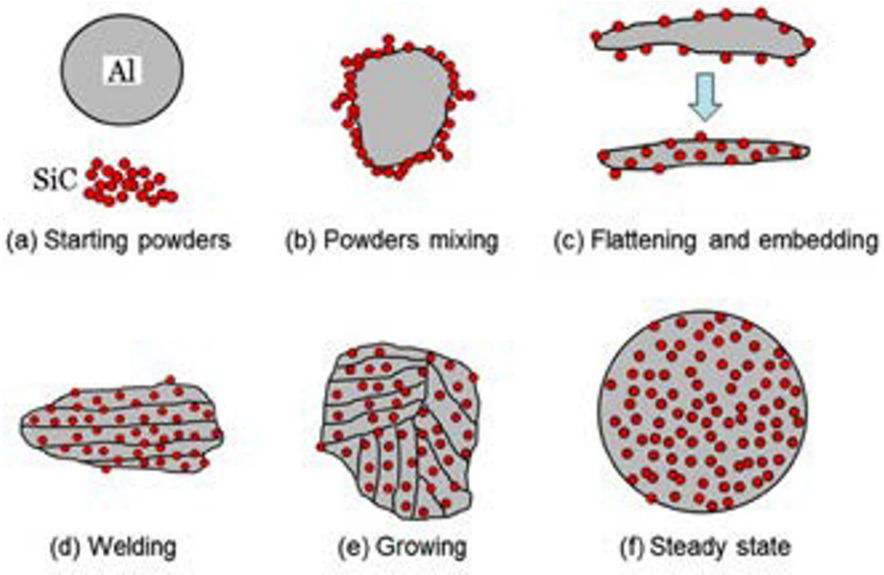

Fig. 5: Various stages of mixture of nano-SiCp and pure Al powder during dry HBM

plastic deformation and finally the mechanical alloying of nano-SiC_p and pure Al was achieved [Fig. 5(e), 5(f)]. At the same time, repeated welding, fracturing and rewelding of lamellar structures would take place due to the heating effect and bending deformation caused by the plastic deformation.

Compared with the long work period of mechanical alloying between Al and SiC_p, the welding of the Al lamellas can be realized more easily due to the high ductility of pure Al and large heating effect of plastic deformation. As a result, some SiC_p were captured by the composite granules in agglomerations, as shown in Fig. 6a. The distribution of nano-SiC_p in the composite granules has significant influence on the dispersion of nano-SiC_p in the melt and the mechanical properties of the final MMNCs. When one-stage HBM was used to fabricate granules, serious agglomeration occured in composite granules and could hardly be broken up by the subsequent ultrasonic vibration (UV) process. To solve this problem, a three-stage HBM process was chosen to make sure that the process of mechanical alloying and the welding of the Al lamellas was completed. Finally, the nano-SiC_p were dispersed uniformly in composite granules as shown in Fig. 6(b).

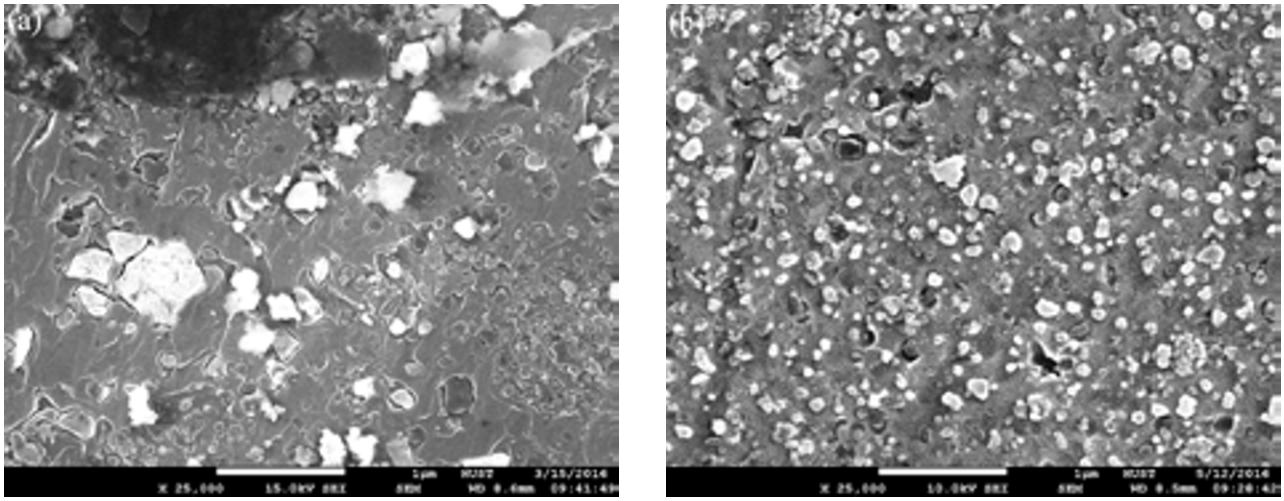

Fig. 6: SEM microstructures of composite granules: (a) one-stage HBM with 300 rpm/15 h; (b) three-stage HBM with 150 rpm/5 h + 200 rpm/15 h + 300 rpm/5 h sequentially

2.3 Microstructure of nano-SiC_p/A356 composites

After the composite granules were added into the melt, nano-SiC_p would diffuse in the melt along with the fusion of composite granules and mechanical stirring. But mechanical stirring was incapable of dispersing the nanoparticles in the melt when the size of composite granules became very small during the melting process. Some areas, as shown in Fig. 7, were found, where the orientation and size of the crystalline grains were quite different from the others due to the pre-dispersion effect caused by the HBM. The content of SiC_p was much higher in these areas, but these areas were too small in size compared with the whole granule and were considered as small agglomerations which might lead to the non-uniformity of MMNCs. The

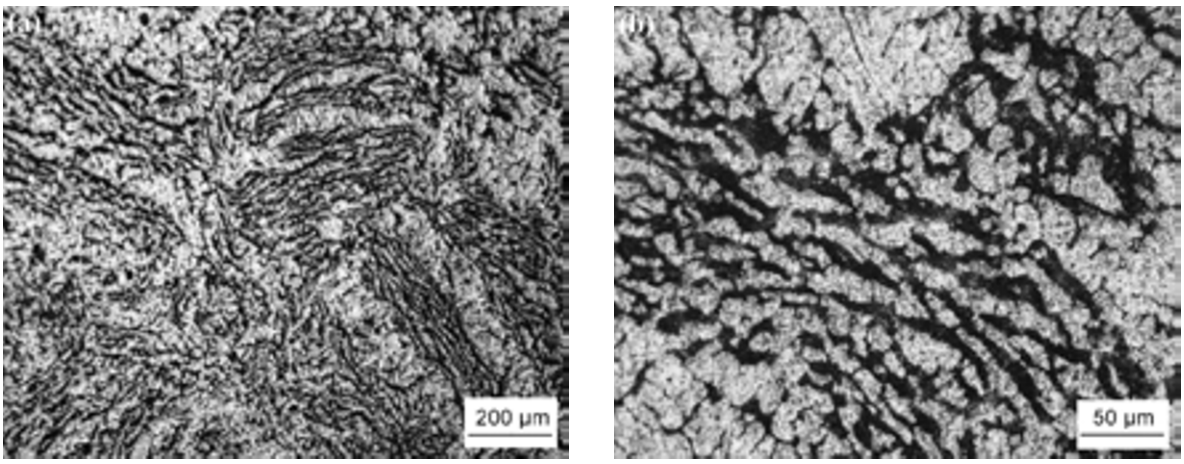

Fig. 7: Agglomeration block of nano-composite without UV at low (a) and high (b) magnification

UV process was taken to break up these agglomerations by the combination effects of transient cavitations and acoustic streaming of UV.

The distribution of SiC nanoparticles of different weight percentage in the aluminum matrix was examined by SEM, as shown in Fig. 8. In addition to the nano-SiC particles, phases of α-Al and eutectic Si were found in the microstructure. Figure 8 shows uniform distribution of nano-SiC particles, and even the small agglomerations mentioned above could not be found in the samples containing different weight percentage of SiC nanoparticles. The breakup of small nano-SiC_p agglomerations and uniform distribution of nanoparticles in the matrix can be mainly attributed to the effect of acoustic cavitation of UV treatment. The implosive collapse of tremendous micro-bubbles induced by the ultrasonic field will generate transient hot spots and form an implosive impact to disintegrate the nano-SiC_p agglomerations. The nano-SiC particles are uniformly dispersed in the melt, and then well distributed in the matrix after solidification.

It is generally recognized that most of the SiC_p would be rejected and pushed out by the growing α-Al phase due to the low wettability between SiC_p and Al crystals, and distributed in the final solidified eutecitc region [15], only a small part of SiC_p can be captured by the growing solid α-Al phase. As shown in Fig. 9(a), the nano-SiC_p distributed in the eutectic region and spontaneously agglomerated in clusters of 100–200 nm in size due to the long solidification duration of the eutectic region.

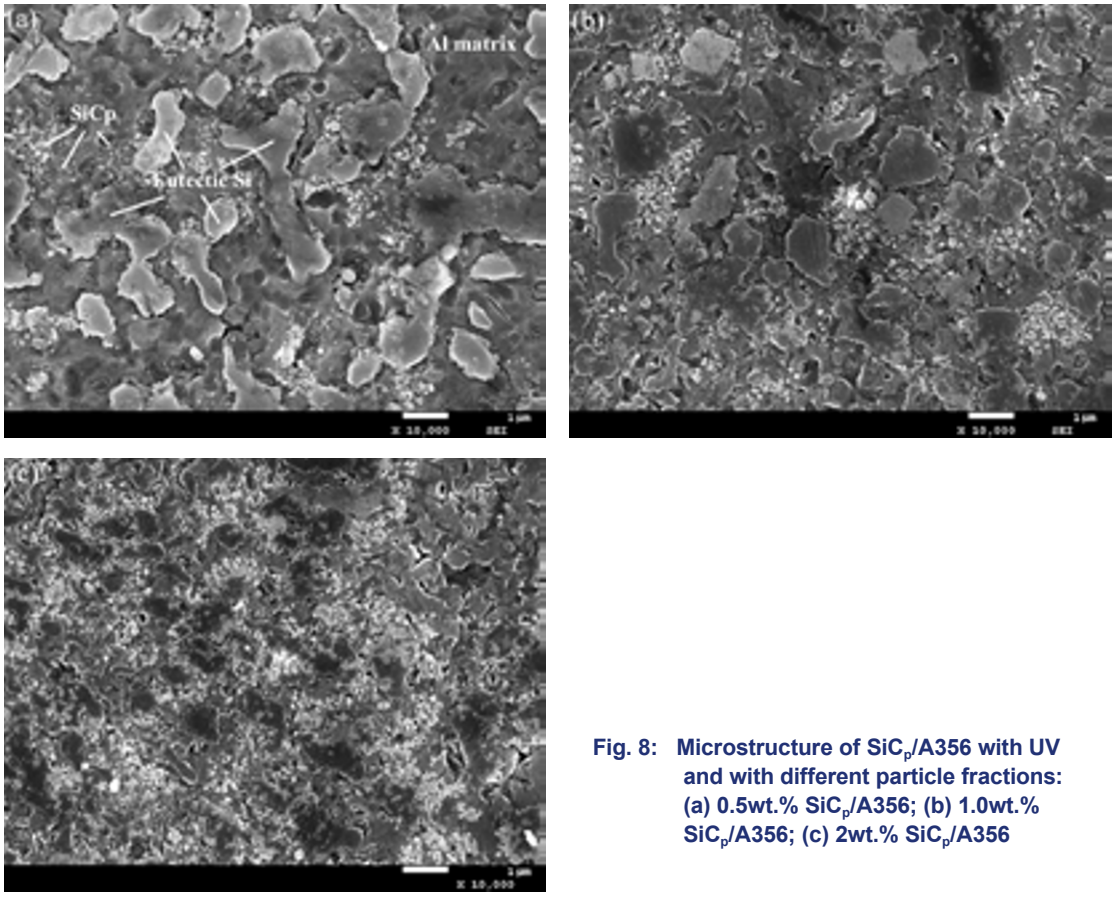

Fig. 8: Microstructure of SiC_p/A356 with UV and with different particle fractions: (a) 0.5wt.% SiC_p/A356; (b) 1.0wt.% SiC_p/A356; (c) 2wt.% SiC_p/A356

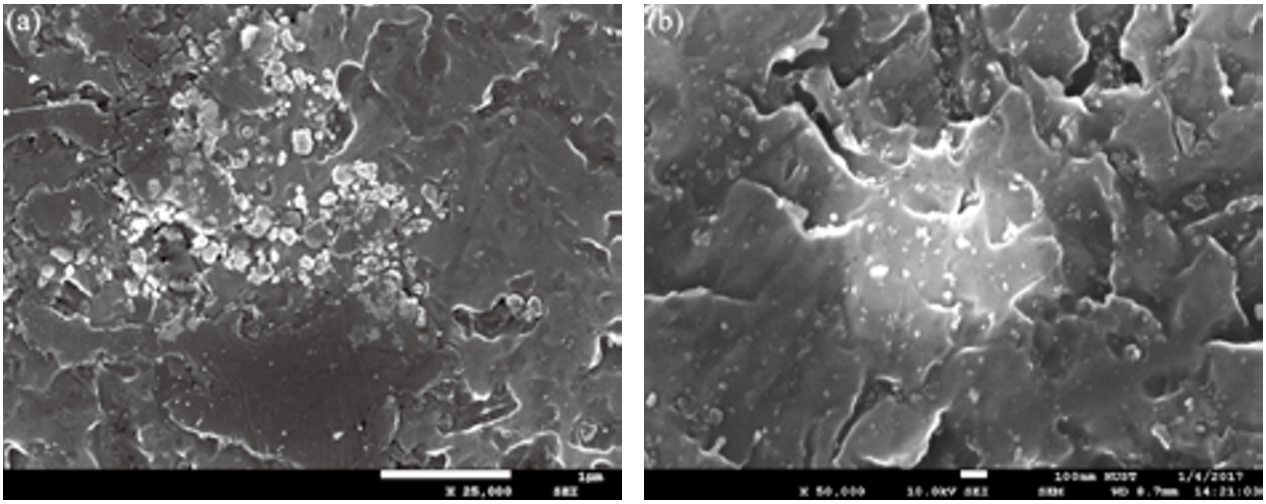

Fig. 9: SEM microstructures of MMNCs with UV: (a) eutectic region, (b) inner of primary α-Al phase

The size of the SiC_p clusters is acceptable and the distribution of nano-SiC_p is good as a whole. Much nano-SiC_p was also found distributed in α-Al crystals, and this kind of distribution, as shown in Fig. 9(b), may be attributed to the interaction between SiO_2 layer on nano-SiC_p and α-Al, and furthur research with TEM is required to confirm the interface combination status.

2.4 Mechanical properties of nano-SiC_p/A356 composites

The room temperature mechanical properties of the composites in as-cast state are given in Table 1. In order to make a comparison, the mechanical properties of the matrix alloy without UV are also listed in Table 1. It can be seen that SiC nanoparticles have good strengthening effects on the aluminium alloy except 0.5%SiC/A356, due to the low content of reinforcement leading to the non-uniformity of the MMNCs. For unreinforced A356 alloy with UV, the mechanical properties were also improved.

Table 1: Mechanical properties of nano-SiC_p/A356 with UV treatment at room temperature

Materials	R_m(MPa)	A(%)
A356 alloy (without UV treatment)	189	3.9
A356 alloy	197	4.2
0.5%SiC/A356	200	5.0
1%SiC/A356	213	5.1
2%SiC/A356	226	5.5

As compared to the A356 matrix alloy, the tensile strength and elongation of the 2.0wt.%SiC/A356 nanocomposites were improved by 19.5% and 43.5%, respectively, in permanent mold casting. It is worth noting that the elongation is also increased simultaneously. This is quite different to the μm-sized SiC_P reinforeced Al-matrix composites, in which the elongation is usually decreased after addition of μm-sized SiC_P. The higher tensile strength could be attributed to the fact that the nano-SiC_p particles act as obstacles to the motion of dislocation, and good distribution of the nano-SiC_p particles and low degree of porosity lead to effective transfer of applied tensile load to the uniformly distributed SiC particulates. On the other hand, nano-SiC_p particles have a refinement strengthening effect, which is further improved with increasing weight fraction since they could hinder the growth of α-Al grains. Refinement of the matrix microstructure results in the increase of the tensile strength and ductility of MMNCs.

3 Conclusions

(1) The mm-sized composite granules containing nano-SiC_p are prepared by HBM, and can be used in a process of solid-liquid mixed casting to fabricate nano-SiC_p/A356 composites. These composite granules with good wettability against Al alloy melt are considered as the carrier agent to make sure that nano-SiC_p can be added into Al alloy melt smoothly.

(2) The nano-SiC_p particles are dispersed well in the matrix and no serious agglomeration is observed, which resulted from ultrasonic vibration for the composite melt before casting.

(3) The tensile strength and elongation of the composites are both increased with the increase of nano-SiC_p fraction, and with 2wt.% nano-SiC_p they are improved by 19.5% and 43.5%, respectively, compared with the A356 alloy.

References

[1] Miracle D B. Metal matrix composites–from science to technological significance. Compos. Sci. Technol., 2005, 65: 2526–2529.
[2] Khosroshahi N B, Mousavian R T, Khosroshahi R A, et al. Mechanical properties of rolled A356 based composites reinforced by Cu-coated bimodal ceramic particles. Mater. & Design, 2015, 83: 678–685.
[3] Si Y, You Z, Zhu J, et al. Microstructure and properties of mechanical alloying particles reinforced aluminum matrix composites prepared by semisolid stirring pouring method. China Foundry, 2016, 13(3): 176–181

[4] Zhang L, Qiu F, Wang J, et al. High strength and good ductility at elevated temperature of nano-SiC_p/Al2014 composites fabricated by semi-solid stir casting combined with hot extrusion. Materials Science and Engineering: A, 2015, 626: 338-344.
[5] Kalaiselvan K, Murugan N, Parameswaran S. Production and characterization of AA6061–B4C stir cast composite. Mater. & Design, 2011, 32: 4004–4010.
[6] Tavoosi M, Karimzadeh F, Enayati M H, et al. Bulk Al–Zn/Al2O3 nanocomposite prepared by reactive milling and hot pressing methods. J. Alloy Comp., 2009, 475: 198–204.
[7] Goujon C, Goeuriot P. Influence of the content of ceramic phase on the precipitation hardening of Al alloy 7000/AlN nanocomposites. Materials Science and Engineering: A, 2003, 356: 399–404.
[8] Hassan S F, Gupta M. Development of high performance magnesium nanocomposites using solidification processing route. Mater. Sci. Technol., 2004, 20: 1383–1388.
[9] Mousavian R T, Khosroshahi R A, Yazdani S, et al. Fabrication of aluminum matrix composites reinforced with nano-to micrometer-sized SiC particles. Mater. & Design, 2016, 89: 58–64.
[10] Tahamtan S, Halvaee A, Emamy M, et al. Fabrication of Al/A206–Al_2O_3 nano/micro composite by combining ball milling and stir casting technology. Mater. & Design, 2013, 49: 347–354.
[11] Su H, Gao W L, Zhang H, et al. Study on preparation of large sized nanoparticle reinforced aluminium matrix composite by solid–liquid mixed casting process. Mater. Sci. Technol., 2012, 28: 178–184.
[12] Lee J, Byun J, Oh C, et al. Effect of various processing methods on the interfacial reactions in SiC_p/2024 Al composites. Acta Mater., 1997, 45: 5303–5309.
[13] Liu J Y, Liu Y, Liu G Q, et al. Oxidation behavior of silicon carbide particles and their interfacial characterization in aluminum matrix composites. The Chinese Journal of Nonferrous Metals, 2002, 12: 961–967.
[14] Fogagnolo J B, Velasco F, Robert M H, et al. Effect of mechanical alloying on the morphology, microstructure and properties of aluminium matrix composite powders. Materials Science and Engineering: A, 2003, 342: 131–137.
[15] Xu J Q, Chen L Y, Choi H, et al. Theoretical study and pathways for nanoparticle capture during solidification of metal melt. J. of Physics: Condensed Matter., 2012, 24: 255–262.

This work was financially supported by the National Natural Science Foundation of China (No. 51574129) and Technological Innovation Special Project of Hubei Province (No. 2017AAA110).